Experimental testing and numerical simulations for life prediction of gate valve O-rings exposed to mixed neutron and gamma fields

D. Battini [a,*], G. Donzella [a], A. Avanzini [a], A. Zenoni [a,b,c], M. Ferrari [a,c], A. Donzella [a,c], S. Pandini [a,b], F. Bignotti [a,b], A. Andrighetto [d], A. Monetti [d]

[a] Dipartimento di Ingegneria Meccanica e Industriale, Università degli Studi di Brescia, Via Branze 38, I-25123 Brescia, Italy
[b] Consorzio Interuniversitario per la Scienza e Tecnologia dei Materiali INSTM, Unità di Ricerca di Brescia, Via Branze 38, I-25123 Brescia, Italy
[c] Istituto Nazionale di Fisica Nucleare, Via Bassi 6, I-27100 Pavia, Italy
[d] Laboratori Nazionali di Legnaro dell'INFN, Viale dell'Università 2, I-35020 Legnaro, PD, Italy

HIGHLIGHTS

- Study of mechanical properties evolution of EPDM irradiated with neutron and gamma mixed fields at different dose levels.
- Identification of structural and functional O-Ring end-points as function of the absorbed dose level (service time).
- Study of the sealing performance of the target chamber gate valve in a new generation radioactive ion beam source.
- Definition of gate valve O-Ring life prediction map as function of service time, storage time and squeeze degree.

GRAPHICAL ABSTRACT
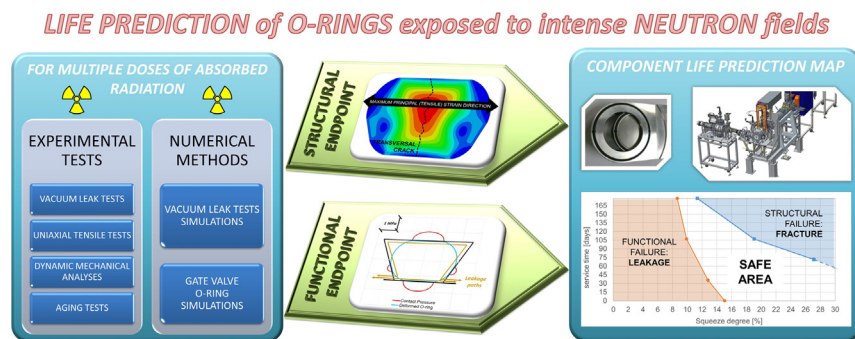
ARTICLE INFO

ABSTRACT

EPDM O-rings of gate valves employed for the construction of a second-generation accelerator for the production of neutron-rich Radioactive Ion Beams were studied in order to assess their sealing performance both during the facility service time and the post-service storage phase. Several O-ring specimens were at first exposed to different dose levels of mixed neutron and gamma radiations. Correspondent modifications of physical and mechanical properties of the material were investigated by means of uniaxial tensile tests, dynamic mechanical analyses, aging, compression set and vacuum leak tests. A hyperelastic strain energy function was adopted to fit the mechanical response of the material as a function of the absorbed dose. The minimum squeeze degree that guarantees O-ring sealing efficiency at different irradiation levels was determined by varying the interference between O-rings and grooves. A finite element model of the vacuum leak test was then set up to assess the contact pressure level required to ensure sealing. Numerical simulations of the gate valve main O-ring were subsequently carried out. By comparison of the predicted contact pressure and strain levels with experimental results, a life prediction map, as function of the service time, the storage time and the O-ring squeeze degree, was proposed.

1. Introduction

The selective production of exotic species (SPES) facility at the Legnaro National Laboratories of INFN [1] is a second-generation accelerator for the production of neutron-rich Radioactive Ion Beams (RIBs).

* Corresponding author.
E-mail address: davide.battini@unibs.it (D. Battini).

The radioactive nuclear species are produced by fission of a ^{238}U target induced by an intense proton beam. The core of the system is the Target & Ion Source (TIS) complex, commonly referred to as target chamber, which houses the target, where fission occurs, and the ion source in a high vacuum environment. Materials and components employed for the construction of the SPES TIS are exposed to a highly radioactive environment, with neutron and gamma fields whose fluxes around the target are of the order of 10^{10} particles/(cm^2 s) [2]. High levels of absorbed dose may induce deep modifications of their physical and mechanical properties, possibly causing loss of their function, or even failure. For precautionary purposes, the uptime of TIS is thus currently set at 15 days. At the end of this life cycle, the exhausted TIS is removed. Due to its very high levels of residual radioactivity, it is transferred, with an automatic handling system, in a shielded repository. Exhausted TIS storage is foreseen to last five years, being the necessary cooling time to reduce the residual radioactivity below specific activity threshold, in accomplishment with radiation protection regulation. In order to carry out this automated removal, valves are required to isolate the TIS and prevent the release of radioactive contaminants in the storage environment. Specifically, two gate valves are used, one corresponding to the Radioactive Ion Beam (RIB) exit pipe and the other one connected to the entering Proton Beam Pipe (PPB), as shown in Fig. 1.

High sealing performance must be guaranteed during the facility uptime (short term functionality) and post-service storage (long term functionality). The use of elastomeric O-rings in such a harsh environment represents one of the most critical aspects of the whole system. Gate valves are equipped with elastomeric O-rings which might undergo premature damage or leakage due to the degradation caused by temperature and radiation effects.

In fact, elastomers suffer from environmental effects that modify their structure and that consequently change their mechanical behavior [3,4]. The radiation damage of these materials has been studied in the past. Nevertheless, results achieved using γ radiation only are reported in the literature. Among the most significant existing investigations, Burnay et al. [5] analyzed the behavior of VITON™ O-rings by means of sealing force measurements, Compression Set tests and leak tests. Their results showed a significant reduction in the sealing force as a function of the absorbed radiation dose. A correlation between absorbed dose and Compression Set performance is observed. Placek et al. [6] analyzed EPDM O-rings, detecting an increase in the brittleness of the material and in the compression set values with an increase of the absorbed dose. Lay [7] studied EPDM gaskets aged at high temperature and subsequently irradiated with γ rays, detecting relevant changes only for high doses.

However, the behavior of these seals in the presence of intense neutron fields remains almost unknown; some of the most recent studies are still reporting results for gamma radiation only [8–10]. The effects of neutron radiations on gasket materials and structural components in general are quite undocumented compared to the effects of γ radiations. Especially for polymeric gaskets, modifications of the mechanical behavior might be quite complex and could be highly dependent on the type of radiation damaging the material. In fact, neutron and photon radiation are known to have very different mechanisms of energy release with matter. Generally speaking, every kind of radiation has a determined efficiency in inducing a defined damage. Moreover, different kind of radiation can induce different typologies of damage. This is extensively reported and documented in several fields of the ionizing radiation applications, ranging from radiation biology to dosimetry and detector science. To the authors' knowledge, few neutron damage studies have been accomplished on polymeric materials. Reasons why the effect of mixed neutron and gamma reactor radiation in polymeric materials might differ from that of gamma alone are reported in [11]. However, the modifications induced by fast neutrons in polymeric materials are reported in [12]. The need for further investigation in this field is reported as well in [13].

Furthermore, to the authors' knowledge, studies that have been carried out on radiation resistance of vacuum O-rings have not been merged yet into specific design and maintenance procedures for applications in nuclear facilities. In fact, it is quite usual to consider the working life as the time needed to cause a variation of 25% of the most radiation-sensitive mechanical property [14]. Overall, this approach recognizes the difficulty of assessing how functional or structural failure is altered by radiation and thus simply (and safely) sets the limit on material stability. In fact, it is quite intuitive that the stability of a single mechanical property might not be the best or the only indicator for life predictions. Moreover, the highly aggressive working environment of the mentioned O-rings may require specific settings for mounting (i.e. groove depth and corresponding squeeze degree). Consequently, the need of high contact pressure to guarantee sealing must be carefully balanced with the risk of failure of the degraded material: the higher the squeeze degree, the higher the contact pressure and the stress in the O-ring.

In this context, a life prediction method for gaskets exposed to intense neutron radiation is presented. The proposed method is appropriate for both short and long-term life. A mechanical characterization of the O-ring material was carried out starting from a previous work of Zenoni et al. [2]. Various experimental test data at different irradiation times were investigated: uniaxial tensile tests, compression sets, aging tests, leak tests, dynamic mechanical analyses (DMA). Finite element method simulations based on the collected data were performed as well to define the end points for the main O-ring of the gate valves used to isolate the exhausted TIS. Specifically, both the structural aspect (i.e. failure due to stress/strain state exceeding the strength of irradiated material) and the functional response (i.e. loss of sealing capacity and
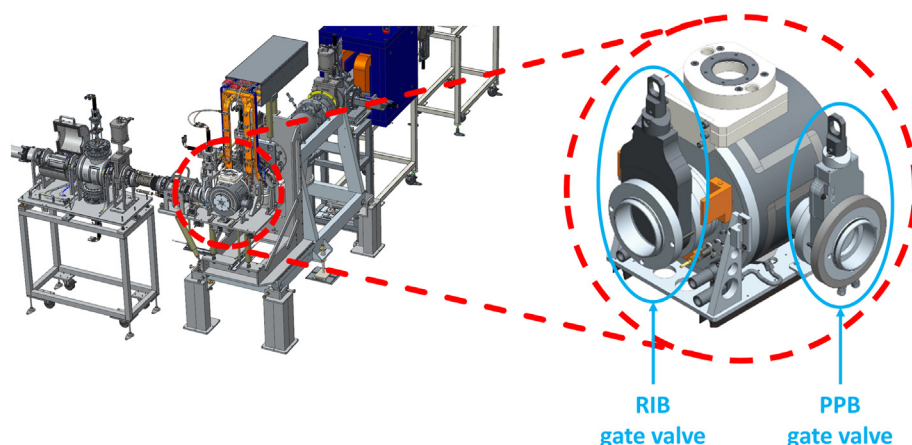

Fig. 1. Scheme of the SPES Front-End where TIS is connected with RIB and PPB pipes. The positions of the two connecting gate valves on the target chamber are shown on the right.

consequent leakage) were considered. Once the working end-points of the customized gate valve currently used in the SPES project were identified, a life prediction map was constructed to summarize our findings in an efficient way.

2. Irradiation conditions and dosimetry calculations

In the SPES facility, the TIS gate valves operate in a mixed neutron and gamma radiation environment. A nuclear irradiation facility was used for materials testing in order to expose the samples to mixed neutron and gamma fields and to replicate the total dose components expected during SPES service. Both the radiation fields present in the testing conditions and in the SPES target are extensively described in [2]. For clarity, a summary is reported in this Section and additional details about dosimetry in mixed fields are provided as well.

2.1. Irradiation conditions in materials testing

O-ring slices of the selected EPDM material were irradiated in the Central Thimble facility of the TRIGA Mark II research reactor of the University of Pavia. The samples were irradiated in an air atmosphere at atmospheric pressure. An extensive measurement campaign was previously performed to characterize the neutron spectrum in the reactor irradiation facilities. In the present work, dosimetry calculations are assessed by means of a simulation of the radiation transport in the reactor irradiation facility using the Monte Carlo simulation code MCNPX [15]. Simulated neutron fluxes showed satisfactory agreement with the measured ones.

A short description of the neutron energy spectrum in the irradiation facility is presented to better explain the mechanism of neutron energy transfer and absorption in EPDM samples. The spectrum is calculated using MCNPX and reported in Fig. 2. The fast component of the neutron spectrum in the irradiation facility originates from fission reactions and it is comparable to a typical fission spectrum. An important thermal neutron component is also present, originating from the moderation processes of fast neutrons which occur in the reactor core and in the reactor fuel elements.

In the presence of such neutron spectrum, the main mechanism of dose release in EPDM is the neutron elastic scattering on hydrogen nuclei. Half of the energy of the incoming neutron is, on average, transferred via elastic scattering to the recoiling proton, which is

responsible for the dose release in the materials [16]. Indeed, in this irradiation condition, the neutron dose is roughly proportional to the hydrogen content. For an accurate simulation of the neutron dose, the hydrogen content was measured with high precision by CHNS analysis for the selected EPDM material [2]. The neutron dose delivered to EPDM via elastic scattering is mainly due to fast neutrons, whereas the amount of energy transferred by low-energy neutrons by the same mechanism is several orders of magnitude lower. Therefore, the dose contribution to EPDM given by the thermal neutron component of the spectrum is negligible. However, all the possible mechanisms of neutron interaction with EPDM are taken into account by MCNPX.

A total dose rate of 700 kGy/h is delivered to EPDM in the Central Thimble facility; the neutron dose rate represents 65% of the delivered dose rate (450 kGy/h), the remaining 35% is gamma dose rate (250 kGy/h). The gamma dose in a nuclear environment is generally underestimated by MCNPX code, since the code is not able to simulate the photons produced by the decay of radioactive fission products [17]. The overall systematic error on the total absorbed dose is estimated to be lower than 15%. It depends on both the error on the neutron spectrum measurements and on an estimation of the fraction of the gamma dose that is not accounted for by the code [17]. The statistical error on the simulated results is negligible compared to the previous systematic ones.

2.2. Irradiation conditions expected during service time

The dose absorbed by the gate valve O-rings in operating conditions is calculated by means of two models of the SPES facility, which are implemented by means of the Monte Carlo codes MCNPX and FLUKA [18]. The use of two different calculation codes was motivated by the need to assess the reliability of the obtained results by a benchmark between two independent codes. The dose components absorbed by the O-rings were simulated during the service time (15 days), during the successive cooling time (15 days) and finally during the storage (5 years).

The neutron spectrum in the TIS gate valve O-rings position reported in Fig. 2 was calculated with MCNPX. In this spectrum, the fast neutrons component is dominant. It originates both from fission reactions and from spallation reactions induced by 40 MeV energy primary protons in the target materials. Due to spallation, this spectrum includes neutrons having energy higher than 10 MeV. By contrast, the typical fission neutron spectrum does not include neutrons having energy higher than
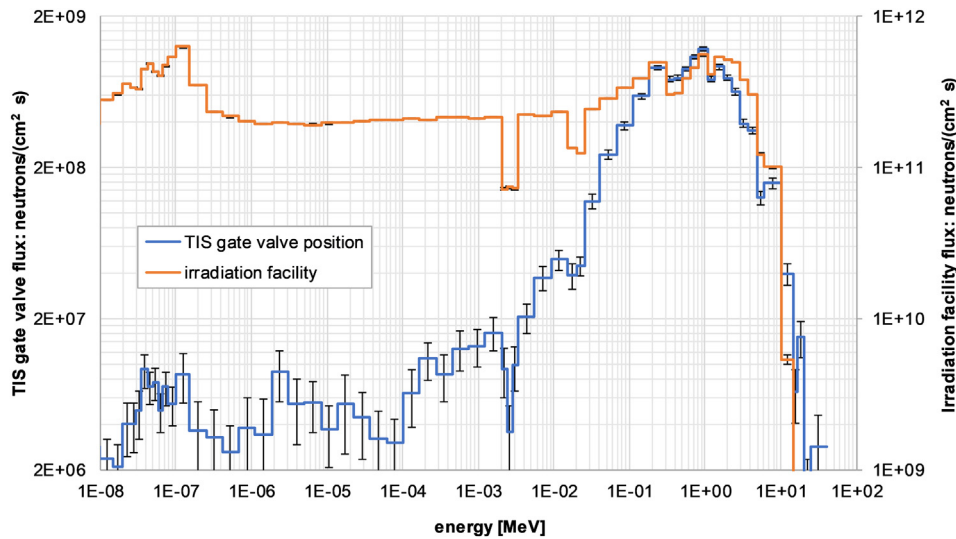

Fig. 2. The neutron energy spectra in the reactor irradiation facility (orange) and in the TIS gate valve position (blue) are reported. The spectra are similar for energies ranging between 0.1 MeV and 10 MeV. The irradiation facility spectrum exhibits a higher component at low energies. The spectrum in the SPES TIS exhibits a component at energies higher than 10 MeV, while in the reactor facility neutrons having such high energy are absent. The spectra are superimposed in the same graph (using different scales) to easily compare their main components and show the good agreement in the 0.1–10 MeV range. (For interpretation of the references to colour in this figure legend, the reader is referred to the web version of this article.)

10 MeV (see Fig. 2). Considering the selected EPDM material, the mechanisms of dose release by fast neutrons are comparable to the ones described for the irradiation facility spectrum.

The dose absorbed by the gate valve O-rings during service time was calculated with MCNPX. A total dose of 300 kGy is delivered to the gate valve EPDM O-rings during this 15-day long time. The neutron dose represents the 85% (255 kGy) of the total and the remaining 15% is gamma dose (45 kGy). The gamma dose component is associated with the prompt gammas produced by fission reactions. The dose component due to the gamma decay of the radioactive nuclides produced in the TIS after the shutdown is not simulated by MCNPX. To calculate this component a FLUKA model of the SPES system was used instead. In this model the gamma dose component was integrated over the fifteen days of cooling time and over the five years of storage. This simulation showed a residual activity of the TIS after the shutdown decaying of about two orders of magnitude during the cooling and of two more orders of magnitude in the first storage year. Thus, the whole additional gamma dose during TIS cooling and storage was estimated to be lower than 5 kGy. This gamma dose was calculated under the assumption that all the radioactive nuclides produced during operation remain confined in the TIS Unit. However, this is a safe (and conservative) assumption since a considerable fraction of the radioactive nuclides produced in the target is extracted from the TIS to be accelerated in the Radioactive Ion Beam line.

Because of the present uncertainties, the error on the simulated dose in operating conditions is about 15%. It is worth highlighting that minor corrections on the absorbed dose values are not expected to significantly influence the results and the methodology described in the present paper.

2.3. Dosimetry in mixed neutron and gamma fields

In the present Section, the most relevant components contributing to the total dose absorbed by EPDM O-rings are considered both for the testing irradiation facility and for the gate valves used in the SPES TIS. Mixed neutron and gamma radiation fields are present in both the situations. These radiation components originate from several types of reactions occurring in the reactor core and in the SPES system. In particular, fission and spallation reactions are the main sources of neutron radiation. Gamma radiation is produced mainly by fission reactions and by the residual radioactivity induced by the primary protons and neutrons produced by fission and spallation reactions. The gamma radiation is also present during the facility shutdown and during the TIS storage due to the decay of radioactive products. The intensity of this gamma radiation decreases with time.

Dosimetry assessments in such mixed fields are particularly complex because of the presence of all the previously mentioned effects. The mechanisms of interaction of neutron and photon radiations with the selected EPDM material are different since they depend on the energy of the radiation. In particular, neutron dose is usually the hardest to be estimated and also to be replicated in testing conditions. In both the considered neutron spectra a consistent fraction of fast neutrons is present, which is the most relevant in delivering dose to the EPDM material. Therefore, the main mechanisms of neutron dose release in EPDM are expected to be very similar in both the considered neutron spectra. For this reason, the neutron component of the dose expected in operation, which is the dominant component of the total dose, is with a satisfactory approximation replicated in irradiation testing conditions. The gamma dose component is comparable in both the irradiation conditions as well.

Concluding, the extensive dosimetry study in both the considered mixed fields allowed the reactor facility to be used to replicate the dose components expected in service conditions. In the present paper, the total amount of absorbed dose (the sum of all the dose components due to different radiations briefly described in this Section) is chosen as

a significant parameter to evaluate the evolution of the mechanical and structural EPDM properties.

3. Mechanical characterization of O-ring material

Different types of elastomeric materials are commercially available for applications as vacuum O-rings, but their behavior in presence of intense neutron fields is not yet completely understood. In a previous study [2], a comparative analysis was conducted on four elastomeric materials: a fluoroelastomer (FPM) and three ethylene propylene diene monomer (EPDM) elastomers. The experimental protocol included irradiation campaigns with neutron and gamma mixed fields at the TRIGA Mark II research reactor of the Laboratory of Applied Nuclear Energy (LENA) of the University of Pavia (Italy), followed by mechanical characterization. The radiation dose delivered to irradiated O-rings in the reactor facility is proportional to the exposure time. Dosimetry calculations in the irradiation facility were completed using a model of the TRIGA Mark II nuclear research reactor [19]. Dose calculations were performed in different positions of the TIS unit as well, where the elastomeric O-rings are employed, using a model of the SPES Front-End [20]. Dosimetry calculations were completed using the Monte Carlo code MCNPX. Duration of irradiation tests at the nuclear reactor were planned, based on the dose rate that can be delivered in its facilities. The goal was to deliver the same radiation levels expected for O-rings during SPES operations but in an accelerated way. More details about dosimetry calculations can be found in [2].

Six irradiation times were considered, as reported in Table 1, along with their corresponding dose levels. After this accelerated aging in radioactive environment, tensile and compression set tests were carried out. Starting from the results from Zenoni et al. [2], the present study carries on further research. Additional experimental tests were performed on elastomers irradiated at the same dose levels as reported in Table 1: temperature aging tests, dynamic mechanical (DMA) tests and leak tests. Moreover, uniaxial data reported in [2] were reprocessed to gather all the needed information. The study of Zenoni et al. [2] concluded that an EPDM based material (peroxide cured) was considered as the best cost-performance choice for sealing applications. For this reason, the present research considered this specific material only, which will be indicated in the following as EPDM.

All the experimental activity presented in the current study is thus carried out on commercial O-rings made of that specific peroxide cured EPDM material. It should be noted that while several information concerning mechanical and physical properties were reported in material datasheet, the exact chemical composition was not disclosed, and no radiation resistance was declared. Of course, this information could help to better understand the mechanisms behind the material property evolution, but the present approach is mainly based on the macro-mechanical response of the material. For this reason, this methodology is potentially adapting to all elastomers, independently from their composition and not necessarily requiring having thorough understanding of material composition and degradation mechanisms.

Since Table 1 shows the direct correlation between irradiation time and absorbed dose level, any of the following data/results in this work will be reported, for convenience, as function of the absorbed dose only.

All the mechanical tests that will be discussed in the following subsections, were carried out at least one month after irradiation occurred on the specimens due to manipulate them safely and avoid any problem related with material activation. In this scenario, since post-irradiation effects may occur, the time elapsed between irradiation and testing

Table 1
Irradiation times in the nuclear reactor irradiation facility and corresponding total dose levels absorbed by the specimens.

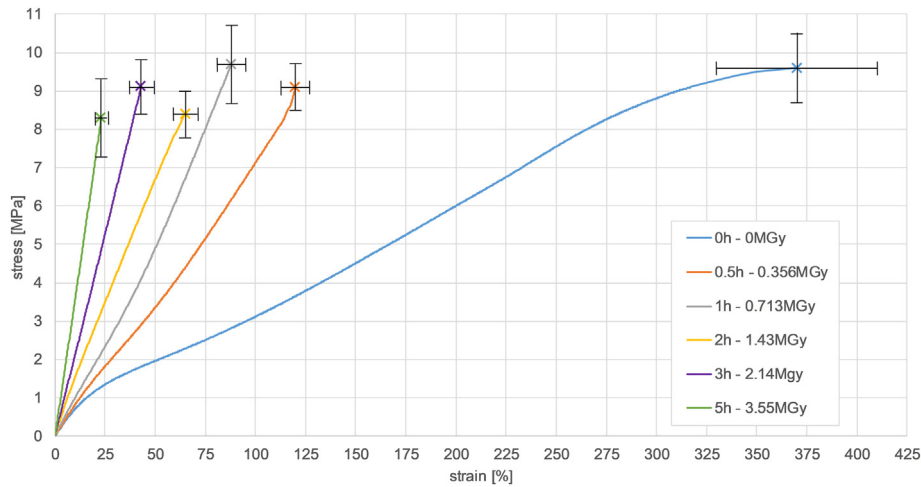| Irradiation time	[h]	0	0.5	1	2	3	5
Absorbed dose	[MGy]	0	0.356	0.713	1.43	2.14	3.55

Fig. 3. Average stress-strain curves of EPDM O-ring samples irradiated at different dose levels obtained from uniaxial test data.

could seem a crucial variable. However, a concurrent experimental activity revealed no sign of oxidation on the material, as shown by FT-IR spectroscopy test on the surface and on the core of the specimens. Moreover, swelling tests and subsequent weight loss measurements after solvent extraction, showed a predominant occurrence of crosslinking, and a limited or decreasing devulcanization and presence of short degraded chains. Finally, for the same level of total absorbed dose, additional experiments were carried out at a lower dose rate (and thus longer irradiation times) and revealed no significant changes of material response on a 10–15 times longer time-scale, indicating no relevant oxidation effects taking place even during a much slower irradiation. This suggested possible oxidation effects being negligible with respect to neutron irradiation effects when considering macroscopical mechanical properties such as stiffness, strain at break, etc.

3.1. Uniaxial tensile tests

Uniaxial tensile tests were carried out on six specimens for each of the six dose levels by Zenoni et al. [2] where all the details concerning the testing conditions are reported. The tests were performed using an INSTRON 3366 testing machine with 10 kN load capacity. The tests allowed the stress-strain correlations for the variously irradiated O-rings to be evaluated.

In the present study, uniaxial tensile data from four tests for each dose level were processed in order to obtain the average uniaxial stress-strain curves. The curves were calculated by averaging the stress values at equal strain levels for the four tests and results are shown in Fig. 3.

The curves reported in the previous figure show an important stiffening effect as the absorbed dose increases.

In addition to stress-strain curves, the most relevant information for the purpose of the present investigation, extracted from all the uniaxial data, are the ultimate properties summarized in Table 2.

Table 2
Ultimate properties of EPDM as a function of the absorbed dose.

Absorbed dose level	Strain at break (avg. ± std. dev.)	Tensile strength (avg. ± std. dev.)
[MGy]	[%]	[MPa]
0	370 ± 40	9.6 ± 0.9
0.356	120 ± 7	9.1 ± 0.6
0.713	88 ± 7	9.7 ± 1
1.43	65 ± 6	8.4 ± 0.6
2.14	43 ± 6	9.1 ± 0.7
3.55	23 ± 3	8.3 ± 1

Particular attention should be paid at the strong influence of the irradiation on the strain at break value of this EPDM: similarly to what Placek et al. [6] detected, the higher the absorbed dose, the more brittle the material. In fact, while the non-irradiated material showed large strains at break, failing at over 320% nominal strain, the most irradiated material became rather brittle, approaching failure along an almost linear stress-strain relationship at only about 23% of the nominal strain. Specifically, the strain at break value was very important as it was considered the limit value for structural integrity. In fact, as it will be discussed in Section 5.2, it is a fundamental input quantity for the proposed O-ring life prediction method.

Since during service time the temperature of the gate valve O-rings rises to approximately 85 °C, aging tests were also performed. To this aim, uniaxial tensile tests were carried out at room temperature on non-irradiated EPDM specimens after a 15-day aging at 100 °C and then compared to non-aged specimens in terms of stiffness and ultimate properties.

Aging tests were carried out on non-irradiated specimens as this condition was associated with the lowest crosslink density and could thus be assumed as the most aging-sensitive condition.

It is possible to observe that the uniaxial stress-strain response at room temperature undergoes to almost no modification after aging as reported in Fig. 4. As a first approximation, the present results can be extended to the irradiated materials as well. In fact, this material showed what can be considered a general stabilization of its properties with irradiation (Zenoni et al. [2]), as phenomenologically testified by an overall stiffening effect and, structurally, by an increased crosslink density.

The curves in Fig. 4 clearly evidence that the prolonged treatment at 100 °C leaves practically unaltered the stress and strain correlation, and the values of stiffness and ultimate properties reported in Table 2, confirms that all the material mechanical properties are maintained after aging.

Anyway, at the present time, one should note that there is no possibility to exclude eventual synergistic effects occurring with a combination of aging and irradiation.

3.2. Compression set tests

Compression set tests were performed according to ASTM D395-03 [21] and ASTM D1414-94 [22] standards on O-ring segments after irradiation at four different absorbed dose levels (see Table 3) during the previous study of Zenoni et al. [2]. The samples were compressed by 25% of the original nominal O-ring cross section diameter and kept under this deformed condition for 24 h at 100 °C. Compression set was measured on the final deformed size, as evaluated at room temperature after unloading and after 30 min relaxation time. Even though the
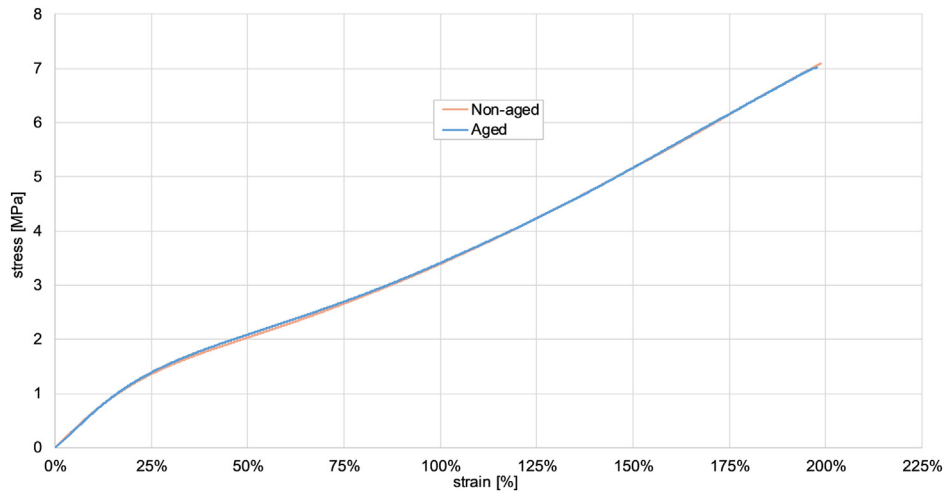
Fig. 4. Aged vs non-aged uniaxial tension data.

Table 3
Compression set test results from Zenoni et al. [2].

Absorbed dose	[MGy]	0	0.356	0.713	1.43	2.14
Compression set (avg. ± std. dev.)	[%]	9.0 ± 0.3	3.9 ± 0.3	5.2 ± 0.3	4.8 ± 0.3	5.4 ± 0.3

results of this test were not directly used to achieve the life prediction of gate valve gaskets, compression set is commonly considered a good indicator of rubber O-ring performance [23–25] and thus they are here reported.

With respect to non-irradiated EPDM, at the lower absorbed dose already, the radiation promotes a significant reduction (and stabilization) of the compression set value, as a probable consequence of the increased crosslinking reaction.

3.3. Dynamic mechanical analysis (DMA) tests

Dynamic mechanical thermal analysis was carried out on rectangular specimens, cut by a sharp razor, from the non-irradiated and variously irradiated O-ring samples. The obtained specimens were rectangular bars, with an average width equal to 5 mm, thickness

equal to 1–2 mm and the gauge length for the test was chosen as 15 mm. The tests were performed by means of a dynamic mechanical analyzer (DMA Q800 - Thermal Instruments), adopting a multifrequency methodology (overall frequency sweep between 100 Hz and 0.4 Hz, with five points per decade) along a heating ramp at 0.5 °C/min from −50 °C to 125 °C.

On the hypothesis of the validity of the time-temperature equivalence and on the application of a time-temperature reduction scheme [26], isothermal storage modulus curves were plotted as a function of frequency for a reference temperature, T_{ref}, of 30 °C. The obtained E' (ω) curves were then expressed as E vs t curves, under the approximation that $E(t) \cong E'(\omega^{-1})$.

The resulting curves are reported in Fig. 5 and clearly show that the main effect of irradiation is to increase the values of the rubbery modulus and the slope of the modulus trend with temperature. These effects are interpreted as a consequence of the increase of the crosslink density.

By contrast, only a slight effect was found on the glass transition temperature T_g, which moves of just few degrees to higher temperatures with higher absorbed doses. Thus, the material behavior at room temperature and above is that of a rubbery material, as shown in Fig. 5, by the sloped plateau for instants above 1 s.
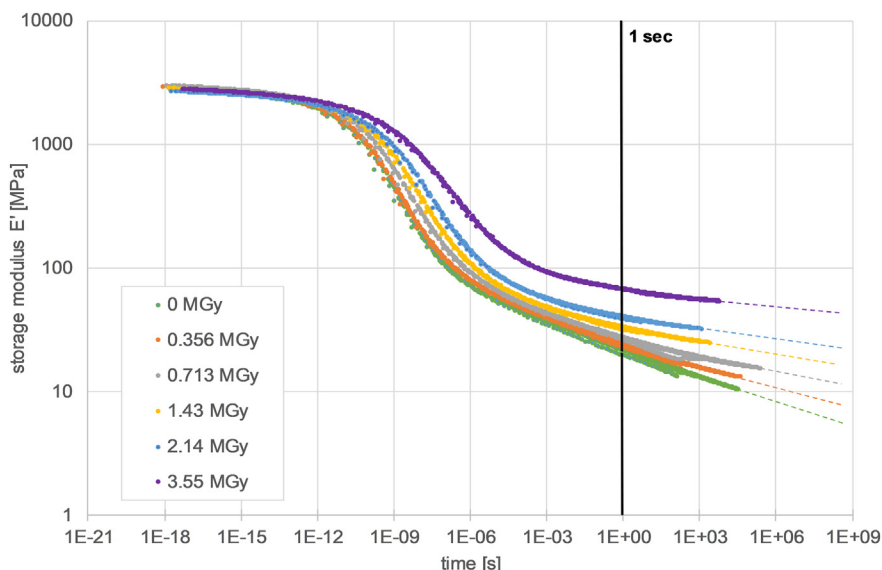

Fig. 5. Master curve for 5 different dose levels (the highest level was not tested). Reference temperature is 30 °C.

Table 4
Slope (k_D) of the linear regression of the rubbery plateau of the master curves from DMA data.

Absorbed dose	[MGy]	0	0.356	0.713	1.43	2.14	3.55
Linear regression slope, k_D	[ ]	−7.08E−02	−5.85E−02	−4.69E−02	−3.74E−02	−3.21E−02	−2.52E−02

Table 5
Different squeeze degrees considering the tested groove depths and reference O-ring dimensions.

Groove depth	[mm]	2.625	2.602	2.562	2.498	2.398	2.098
Squeeze degree	[%]	0.570	1.44	2.84	5.38	9.17	20.5

Fig. 6. Experimental apparatus for Vacuum Leak Test mounted on the HLD.

Since the master curves did not show an ideal rubbery plateau and obtaining experimental test data at longer times was not possible (higher temperature and/or lower frequencies would have been very troublesome to test), an extrapolation at longer times was necessary.

The following equation, representing a linear regression in the log-log domain for higher times, was used:

$$\log_{10}E(t) = \log_{10}E_{1\ sec} + k_D \cdot \log_{10}t \tag{1}$$

where $E(t)$ is the storage modulus as function of time and E_{1sec} is the storage modulus at 1 s. k_D represents the slope of the fitted linear regressions and is reported in Table 4. A time of 1 s was chosen both to only fit the last few decades of the curves and because it was considered a representative time for the uniaxial tests.

It is worth noting that the value of the rubbery plateau slope, k_D, is not dependent on the reference temperature of the master curves since, according to the time-temperature equivalence principle, the effect of temperature is a rigid shift of the master curve along the time scale.

4. Functional characterization of O-ring through vacuum leak tests

Vacuum Leak Tests (VLT) were carried out to determine the minimum squeeze degree to guarantee O-ring sealing efficiency at different irradiation levels. Tests were performed on O-rings with reference dimensions of 2.64 mm for the cross-sectional diameter and 13.94 mm for the internal diameter so that they could be introduced in the irradiation facility of the TRIGA Mark II reactor.

Six different groove depths were chosen between almost no-compression and approximately 20% squeeze degree for the tested O-ring dimensions following the definition of Eq. (2):

$$Squeeze\ degree\ (SD) \stackrel{\text{def}}{=} \frac{d_S - d_{S,m}^*}{d_S} \cdot 100\# \tag{2}$$

where $d_{S,m}^*$ is the compressed minimum cross-sectional diameter and d_S is the undeformed cross-sectional diameter.

As reported in Table 5, most of the tests were carried out at low squeeze degree values to achieve better sensitivity close to the expected leakage initiation O-ring compression.

Four different absorbed doses were chosen: 0 MGy (non-irradiated specimens), 0.713 MGy, 2.14 MGy and 3.55 MGy.

4.1. Vacuum leak tests

Leak tests were carried out using a Helium Leak Detector (HLD) INFICON UL 200 available at the Legnaro National Laboratories of INFN and equipped with a customized holding device for the tested O-rings (See Fig. 6).

The leakage threshold design target value for HLD tests was 5E−07 mbar l/s. This threshold was then used to establish the minimum squeeze degree (SD_{lim}) in order to guarantee a no-leakage condition for each dose level during the VLT.
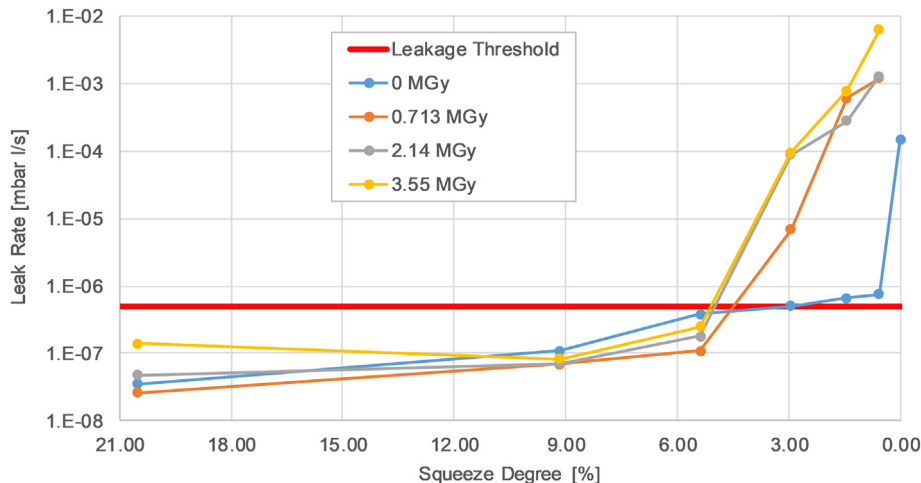

Fig. 7. Leak rates results from VLT.

Table 6
Squeeze degree for leakage initiation. Irradiated specimens show very similar values.

Absorbed dose level	[MGy]	0	0.713	2.14	3.55
Squeeze degree for leakage initiation (SD_{lim})	[%]	2.95	5.24	5.37	5.37

Leak rate results reported in Fig. 7 are shown in logarithmic scale to improve figure readability. Resulting squeeze degrees for leakage initiation are reported in Table 6.

By comparing the leak rate curves and the SD_{lim} values, it can be seen that the main difference in the material behavior occurs between the non-irradiated O-ring and the irradiated ones. In fact, the squeeze degree associated with leakage initiation showed to be almost insensitive to the absorbed dose level, with the exception of the non-irradiated O-rings.

Interestingly, this trend closely reminded that of the compression set tests seen in Section 3.2, where the irradiation effects seem to stabilize the material elastic response (i.e. recovery at unloading), probably due to the increased crosslink density. Thus, it may seem counterintuitive that for a material with an improved elastic response, a worsening in the leak test response is measured. However, this might be explained with the simultaneous increase in material stiffness at higher dose levels, since it is quite reasonable that, independently from the elasticity of the response, the stiffer the material the higher the squeeze degree level to guarantee a no-leakage condition. Moreover, while permanent set and stress relaxation phenomena come into play during compression set tests, since its conditions promote material viscous flow, leakage tests, from which SD_{lim} values are calculated, are carried out on almost non-relaxed specimens. Thus, when doing this comparison, stress-relaxation sensitivity at different absorbed dose levels, as seen in Fig. 5 and Table 4, is not considered. Nonetheless, this sensitivity will instead be crucial when building the life prediction map as discussed in Section 5.4.

No permeability tests were carried out as permeability leakage should be negligible compared to mechanical leakage as described in the report from Yamamoto et al. [24].

4.2. Finite element simulations of the vacuum leak tests

This finite element model is used for replicating the experimental vacuum leak tests in order to gather further data and correlate the contact pressure distribution on the O-rings with the leakage initiation condition.

4.2.1. Model setup

Finite element simulations were carried out with the commercial code Simulia Abaqus 2016 from Dassault Systèmes. An axisymmetric model was used and a static analysis was performed. Groove and O-ring geometries were exactly those of the VLT. The O-ring mesh consisted of roughly 51,600 quadrilateral first order elements (CAX4RH) while the walls were modelled as analytic rigid surfaces

and no mesh was necessary. Typical element dimension in the contact regions was about 7.5 μm to ensure a good accuracy in terms of contact pressure distributions. The O-ring was modelled as hyperelastic and ideally incompressible with a Marlow strain energy formulation which is a function of the first invariant only [27]. For each absorbed dose level, a uniaxial data fit was performed in order to obtain a radiation-dependent mechanical behavior of the EPDM.

Stress relaxation effects were included in the analyses by assuming a time dependency of the stress-strain relationship of EPDM analogous to the long-time trend of the storage modulus resulted from dynamic mechanical analysis (DMA) tests (see Fig. 5). Specifically, the whole stress-strain curves were scaled down following Eq. (3):

$$\sigma_{D,t}(\varepsilon) = \sigma_D(\varepsilon) \cdot t^{k_D} \tag{3}$$

where the exponent k_D (see Table 4) was calculated from DMA data presented in Section 3.3 and the stress-relaxation time (in seconds) t corresponds to the time at which VLT measures were taken. $\sigma_D(\varepsilon)$ is the stress-strain relationship in non-relaxed conditions and the subscripts D identify data at a specific dose level.

Contact interactions were included between the O-ring and the groove walls, assuming a friction coefficient of 0.3 which is a common value for rubber to aluminum contact. However, the analyses showed a totally negligible sensitivity with respect to the value of the friction coefficient. While the groove surrounds the O-ring on three sides, the different squeeze degrees were obtained with a boundary displacement imposed on a mobile wall placed on the fourth side of the O-ring.

The simulation was divided into three steps (see Fig. 8):

1. The O-ring was compressed to reach the desired squeeze degree necessary for the closure.
2. A pressure differential of −1 bar was then applied on the internal surface of the O-ring to simulate vacuum condition in the leakage initiation condition.
3. A stress-relaxation time of 300 s was applied.

The stress relaxation step was necessary to correctly calculate contact pressure distribution since the VLT measures were taken approximately 5 min after the O-ring was compressed. The pressure differential of step 2 was applied on both the top and bottom inner regions of the O-ring (BC and CD arcs, see Figs. 8 and 10) because it was assumed that the leakage on the inner diameter of the O-ring (through point C, see Figs. 8 and 10) would happen before global leakage from outside to inside (through either point B or D, see Figs. 8 and 10). This assumption was well supported by the fact that the contact pressure distribution p_3 (located in C) was always lower than p_2 (located in B) and p_4 (located in D), as it is clearly reported in Fig. 10.

4.2.2. Results

Results of VLT simulations are shown in Fig. 9, where the contact pressure between O-ring and groove and the maximum (positive)
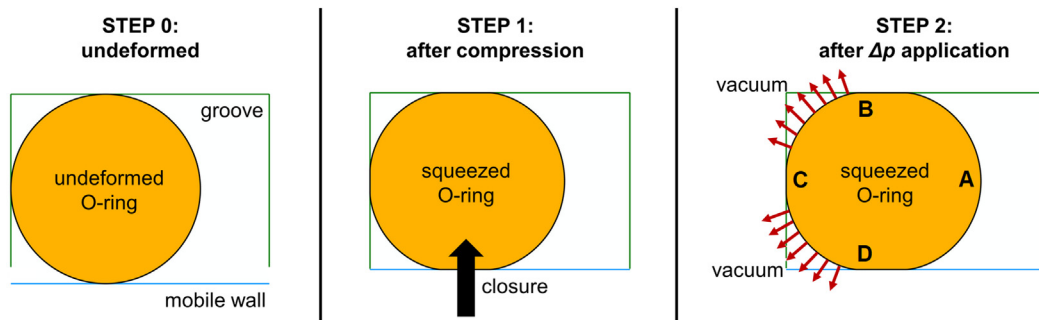

Fig. 8. Schematic representation of VLT assembly as in the finite element software. Step 3 is not shown as it is a change in material properties and not in boundaries or loads.
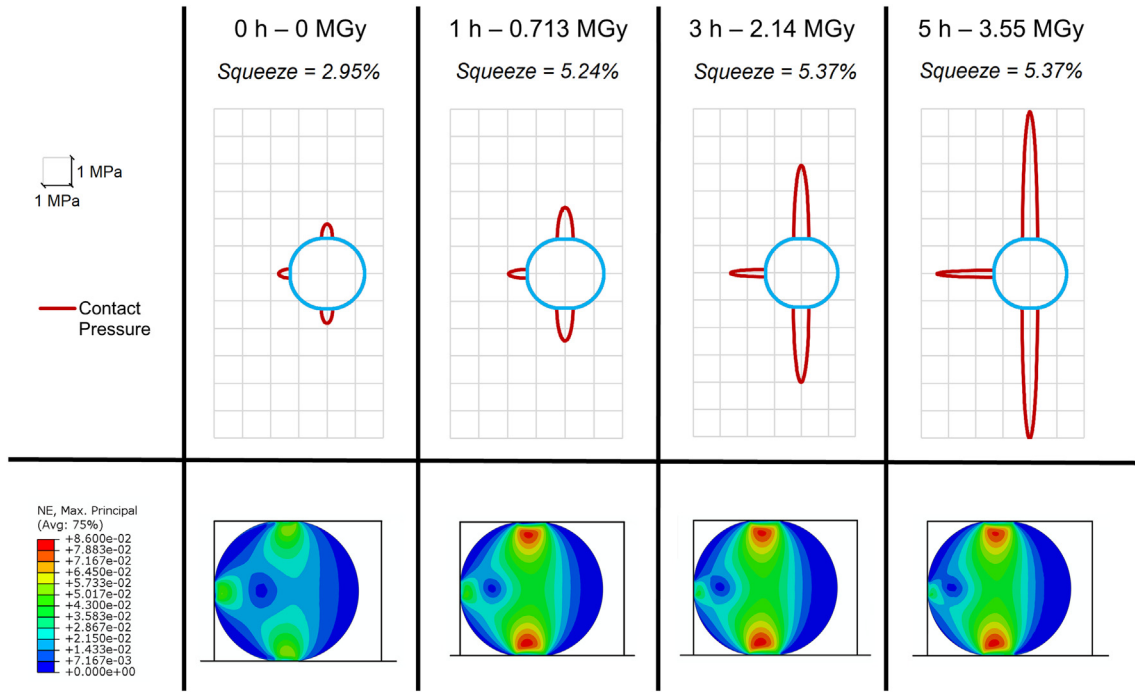
Fig. 9. Results for the FEM simulations of the leakage initiation condition of the VLT. On top, the contact pressure is plotted on the deformed O-ring profile. Contour map of the maximum (positive) principal nominal strain is reported below. Every result is reported for the four absorbed dose levels used for the leak tests.

nominal strain contour in the O-ring as function of the absorbed dose level are reported.

From Fig. 9 we can observe that the peak value for the maximum (positive) principal nominal strain is related to the squeeze degree only, as expected. In fact, for 0.713 MGy, 2.14 MGy and 3.55 MGy

absorbed dose levels, the contour maps were very similar to each other since the applied squeeze level (see Table 6) were also very similar for these three cases. Moreover, the peak of the maximum (positive) principal nominal strain was located close to the contact regions because the applied squeeze degree was quite low.

On the other hand, contact pressure distributions showed to be very sensitive to the absorbed dose as the material became noticeably stiffer at higher dose levels.

4.3. Limit contact pressure (p_{lim}) calculation

By combining experimental results of VLT and contact pressures predicted by VLT FEM model, a limit contact pressure p_{lim}, associated with leakage initiation, was calculated. For the examined configuration there were two possible leakage paths and a total of four possible contact points (see Fig. 10). A definition of p_{lim}, totally independent from groove shape and geometry, can be assumed as per Eq. (4):

$$p_{lim} \stackrel{def}{=} \min(\ \max(p_1, p_2, p_3),\ \max(p_4)) \tag{4}$$

where p_i are the contact pressure distributions on the four sides of the O-ring (for this specific test condition there was no contact on side 1, p_1 was null, see Fig. 10).

Values of p_{lim} determined according to this definition are summarized in Table 7. The limit pressure p_{lim} is a very important quantity as it is a more general indicator of leakage initiation condition compared to the previously, experimentally determined, limit squeeze degree SD_{lim}. It was also quite evident that, differently from SD_{lim}, p_{lim} assumed a clearly monotonic trend. Since the material became stiffer at higher absorbed dose levels, the required contact pressure to ensure the same fit at a microscopic scale between O-ring and groove also
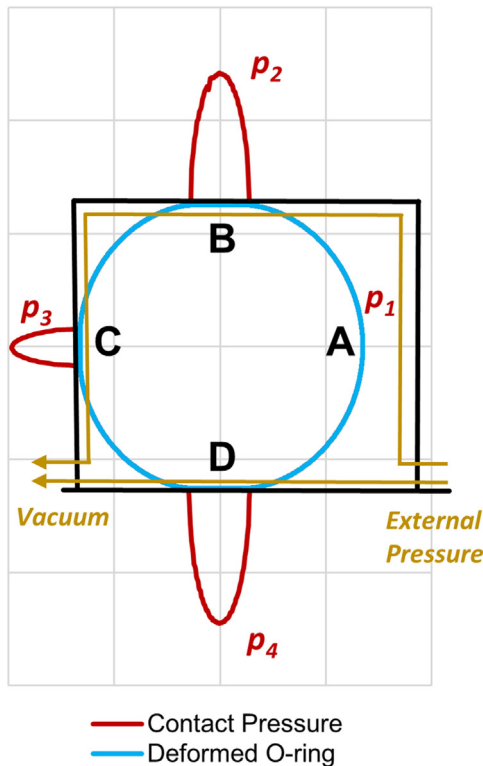

Fig. 10. Example (corresponding to the 0.713 MGy absorbed dose of the previous figure) of a deformed configuration from VLT simulation with contact pressure distribution and the two possible leakage paths.

Table 7
Limit contact pressure for leakage initiation.

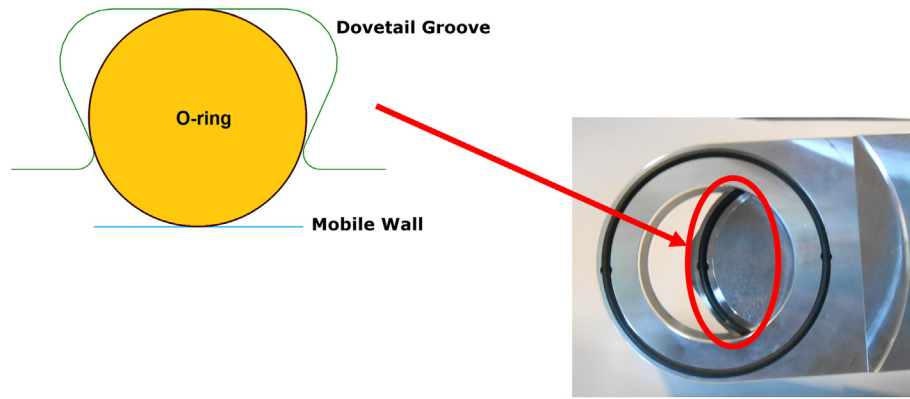| Absorbed dose level	[MGy]	0	0.713	2.14	3.55
p_{lim}	[MPa]	0.52	1.15	2.66	4.62

Fig. 11. Main O-ring of the gate valve. Schematic representation of the O-ring assembly for the finite element simulation on the left and representative image of the real component on the right.

increased. In fact, ideally, the leakage is prevented when the sealing material fills both the cavities and the irregularities of the groove.

As it will be discussed in Section 5.2, p_{lim} is a fundamental input parameter for O-ring life prediction.

5. Gate valve O-ring life prediction

Gate valves might be used in many different designing scenarios and environments. Usually they are not well suited for flow regulation, as the associated turbulence might be a serious issue. On the other hand, these valves are a good choice for permitting or preventing fluid flow since they are quite compact allowing better design optimization of the piping. They also guarantee very low friction when fully opened and they are reliable thanks to the "simple" design and functioning.

Specifically, in the examined case, two gate valves are used to isolate the TIS and prevent the release of radioactive contaminants during the storage phase. Investigations of the structural and functional end points were carried out for the main and most critical O-ring of the valve which is the one located on the shutter (see Fig. 11).

5.1. Finite element simulations of the gate valve

FEM simulations of the gate valve main O-ring were carried out in order to gather all the necessary data to calculate the end points for both the working and the storage condition.

5.1.1. Model setup

A scheme of the assembly as in the FEM software is provided in Fig. 11, along with a representative image of the gate valve.

Groove and O-ring geometries were obtained from measurements on the customized gate valve adopted for the SPES project and from the standard dovetail grooves dimensions as classified by the Aerospace Standard AS568A. Specifically, the cross-section and the internal diameters of the O-ring were, respectively, 3.34 mm and 102 mm. The model setup in terms of boundary conditions, element type, interaction definitions and mechanical behavior of the material was identical to the one described in Section 4.2.1. The simulation was divided into four steps:

1. The O-ring was inserted in the groove (O-ring placement).
2. A variation of material properties was applied to simulate material modifications during service time to consider radiation dependency of the EPDM properties.
3. The O-ring was compressed to reach the squeeze degree at gate valve closure at the end of the service time.
4. A variation of material properties was applied to consider stress-relaxation phenomena that take place during the storage phase.

The applied absorbed dose level for step 2 followed from proper dosimetry calculations on the model reported in [20]. Dosimetry calculations were carried out on the exact location of the RIB gate valve which resulted the most irradiated gate valve of the system. Its absorbed dose was 0.3 MGy for a 15-days long service time. The stress-relaxation time applied in step 4 corresponded to the storage time.

The analyses were carried out at 0, 17.8, 35.6, 71.5, 107, 177 days of service time, corresponding to the six absorbed dose levels used for tensile tests. For each service time, the applied storage times were 0, 1, 7, 30 days and 1, 5, 10 years. For each of the 42 combinations of service and storage time, the applied squeeze degree varied from 0 to 30% with very small steps in order to achieve a satisfactory sensitivity on the results and avoid interpolations. No pressure differential was applied since the venting phase of the SPES system involves the pumping of Argon gas inside the TIS and the vacuum conditions are removed before the TIS is isolated by the gate valves and moved to the storage area.

In the end, all the necessary results for life prediction could be extracted for each parameter combination (squeeze degree, service time, storage time) to estimate the short (end-of-service) and the long-term (end-of-storage) conditions assuring O-ring integrity both from a structural and a functional point of view.

5.1.2. Results

Selected results for the finite element simulations of the gate valve are shown in Fig. 12. A sample of 18 combinations of parameters is reported: 6.7%, 13.5% and 20% squeeze levels, 0 and 37 days service times, and 0 days, 30 days and 5 years storage times.

The peak value of the maximum (positive) nominal principal strain showed to be almost insensitive to the service time, as it was to be expected in a geometrically bounded configuration. As it can be appreciated from Fig. 12, the location of the peak value moved from the subsurface close to the contact areas towards the center of the O-ring as the squeeze degree increased, because the O-ring transversal stretch became predominant.

As expected, the contact pressure distribution peaks decreased at higher storage times due to stress-relaxation phenomena and increased both at higher squeeze degrees and at higher irradiation levels. The contact pressure distributions on the inner and outer diameter of the O-ring (respectively p_3 and p_1) came into play at higher squeeze degree only. Nevertheless, their peak values remained lower than those of the top and bottom pressure distributions (p_2 and p_4) for any squeeze degree as it can be appreciated in Fig. 13.

5.2. Procedure for life estimation of O-rings

In order to turn all the reported results in a quantitative tool for lifetime predictions, end-points for structural and functional failure had to be defined.
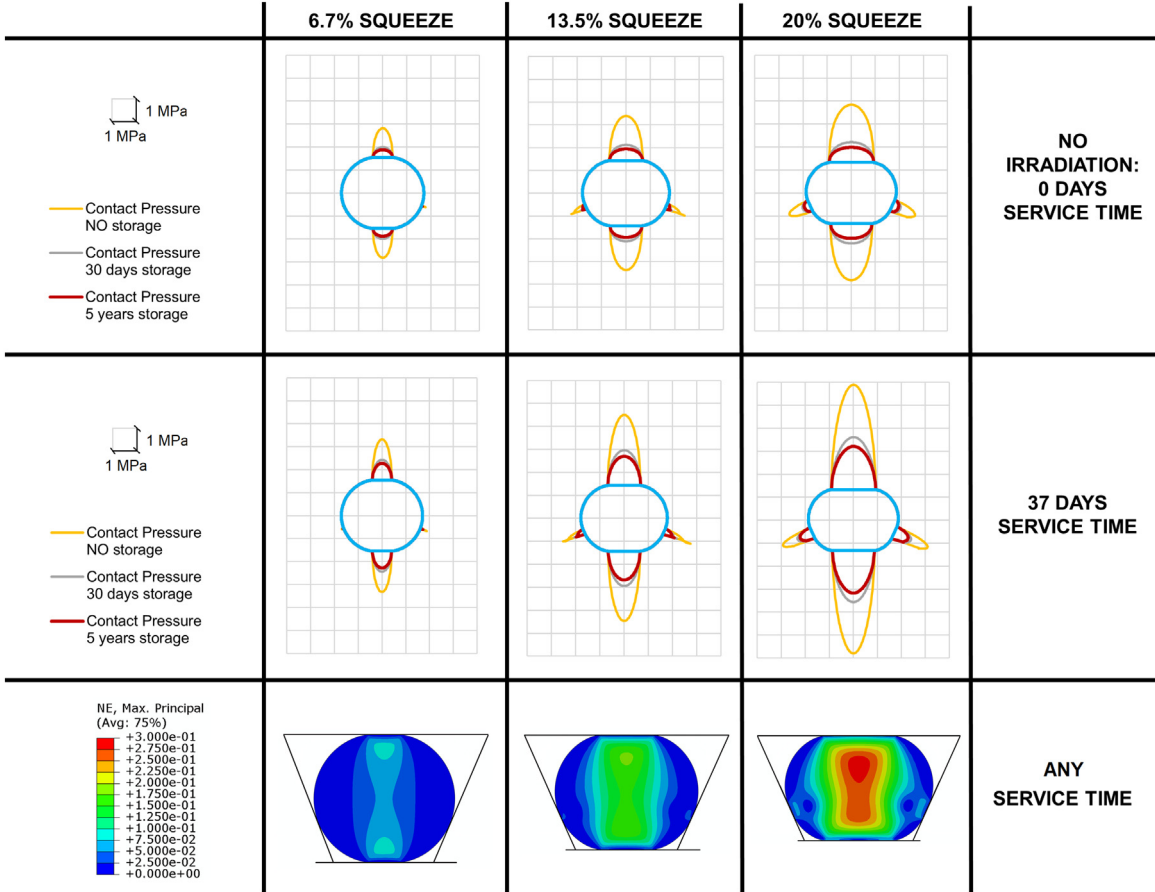
Fig. 12. A sample of results for the FEM simulations of the gate valve. Three squeeze degree levels, three storage times and two service times are shown. On the top rows, contact pressures are plotted on the deformed O-ring profile. Contour maps of the maximum (positive) principal nominal strain are reported at the bottom of the image.

5.3. End-point calculation

To this aim, the end-points could be generally described as:

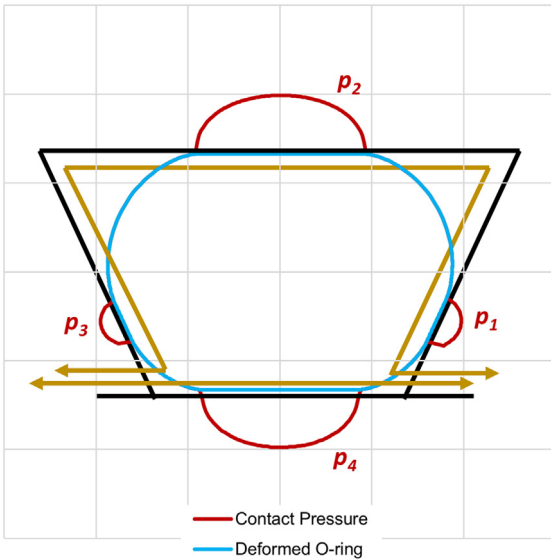$$EP \stackrel{\text{def}}{=} \frac{FI}{FI_{adm}} \tag{5}$$

Fig. 13. Possible gas flow on the main O-ring of the gate valve. Gas might leak in both direction as a pressure gradient is not applied over the O-ring section.

where EP is the end-point, FI is the failure indicator quantity and FI_{adm} indicates the admissible value for this failure indicator. Thus, if EP ≥ 1 then the end-point has been reached and if EP < 1 then functioning of the system is preserved.

Regarding the structural aspect, a brittle fracture was assumed as the failure condition because the higher the radiation the more fragile the mechanical behavior of this EPDM, as also noticed from failures occurred during compression set tests (see Fig. 14). For this reason, the peak value of the major principal (tensile) strain was considered a good failure indicator FI_s. In fact, while the minor axis direction of the deformed O-ring cross-section showed mostly compressive strains, the major axis direction showed mostly tensile strains.

$$FI_S \stackrel{\text{def}}{=} \max(\varepsilon_I) \Rightarrow FI_{S,adm} \stackrel{\text{def}}{=} \text{Inf}(\varepsilon_{I,break})_{99\%} \tag{6}$$

The strain at break can then be considered the limit value for the structural failure indicator and the admissible value was thus defined as follows:

$$FI_{S,adm} \stackrel{\text{def}}{=} \text{Inf}(\varepsilon_{I,break})_{99\%} \tag{7}$$

where $\text{Inf}(\varepsilon_{I,break})_{99\%}$ is the lower bound of the strain at break with a 99% confidence obtained by applying a Student's *t*-distribution. Results are reported below (Table 8).

Following these definitions, it is quite evident that while $FI_{S,adm}$ is a function of the absorbed dose level only, FI_s is a function of the squeeze degree and the behavior of the material.

Similarly, in order to evaluate potential lack of sealing, a functional failure indicator (FI_F) had to be defined. To this aim, following [28], we considered the value of contact pressure at the interface between
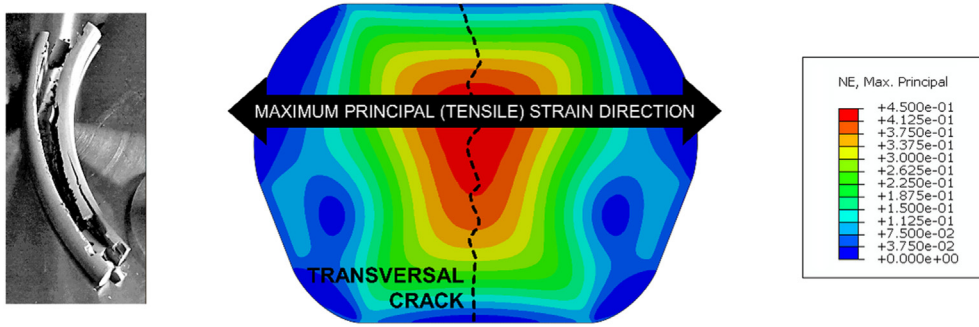
Fig. 14. On the left, experimental evidence of brittle fracture on O-rings during compression set tests. On the right a vectorized map of the maximum principal nominal strain.

Table 8
Admissible values for the structural failure indicator.

Absorbed dose	[MGy]	0	0.356	0.713	1.43	2.14	3.55
$\varepsilon_{l, break}$ (avg. $\pm$ std. dev.)	[%]	370 $\pm$ 40	120 $\pm$ 7	88 $\pm$ 7	65 $\pm$ 6	43 $\pm$ 6	23 $\pm$ 3
$FI_{S, adm}$	[%]	245	103	67.2	46.7	27.0	14.3
Reduction			−34%	−17%	−24%	−28%	−38%	−39%

groove walls and O-ring, which is a function of interference fit, geometry of the groove and mechanical behavior of the material. Considering our sealing configuration, this quantity corresponded to the limit contact pressure p_{lim} previously calculated in Section 4.3:

$$FI_F \overset{\text{def}}{=} \min(\ \max(p_1, p_2, p_3),\ \max(p_4)) \Rightarrow FI_{F,adm} \overset{\text{def}}{=} p_{lim} \qquad (8)$$

In the end, analogously to the structural failure indicator, $FI_{F,adm}$ is only a function of the absorbed dose level, while FI_F is a function of both the squeeze degree and the behavior of the material (both in terms of absorbed dose level and stress-relaxation time).

5.4. Life prediction map

At this point, the life prediction map could be constructed as both the end-points were totally defined. The maps were obtained by overlapping the failure areas identified by both the end-points considering the usage of admissible values ($FI_{S, adm}$ and $FI_{F, adm}$) and the free surface of the map corresponds to the safe area.

The end-points were not only functions of the absorbed dose level and the squeeze degree but also of the stress-relaxation time, which corresponds to the storage time. For this reason, the life prediction map could still be expressed as function of service time and squeeze degree but multiple curves delimiting the functional failure area existed: one for each simulated storage time. Of all the FEM simulations, those at 0.356 and 1.43 MGy absorbed dose levels were excluded from the procedure to build the functional end-point curves since leak test data, and thus $FI_{F, adm}$ values, were not available at those specific levels. The resulting life prediction map is shown in Fig. 15.

This life prediction map clearly shows how critical is the combination of the three parameters of interest (squeeze degree, service time and storage time) in terms of safe area definition.

In particular, the functional end-point shows a high sensitivity to the storage time due to the huge impact of stress-relaxation phenomena on the contact pressure distribution. The higher the storage time, the lower the contact pressure and thus the more extended the functional failure area. Moreover, it is very interesting to notice how the curves describing the functional end-point change from monotonically increasing to monotonically decreasing because of the different sensitivity to stress-relaxation shown by the material at different absorbed dose levels. This can also be looked as the fact that the material behavior becomes progressively more crosslinked, and the increased network density slows down relaxation process.

For the same reason, it is also worth showing with Fig. 16 that the compression set and the functional end-point at 10 years of storage time, have a similar trend with respect to the absorbed dose level, while the trend is inverse when considering the functional end-point
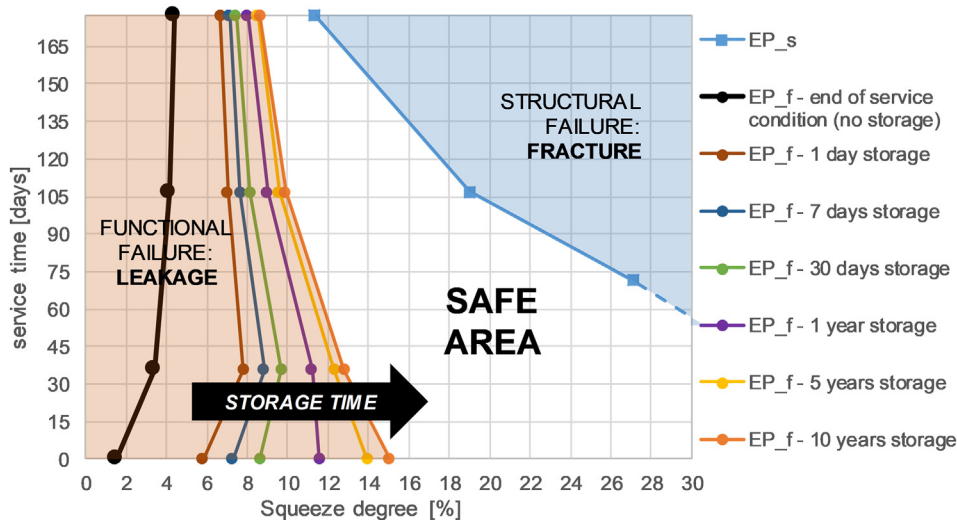

Fig. 15. Life prediction map of main gate valve O-ring. Multiple curves are shown for the functional end-point to represent various storage times. Functional failure area was filled to the longer storage time as this was the most limiting condition. The lower part of the structural end-point curve is shown as dotted since it resulted from strain at break data interpolation.
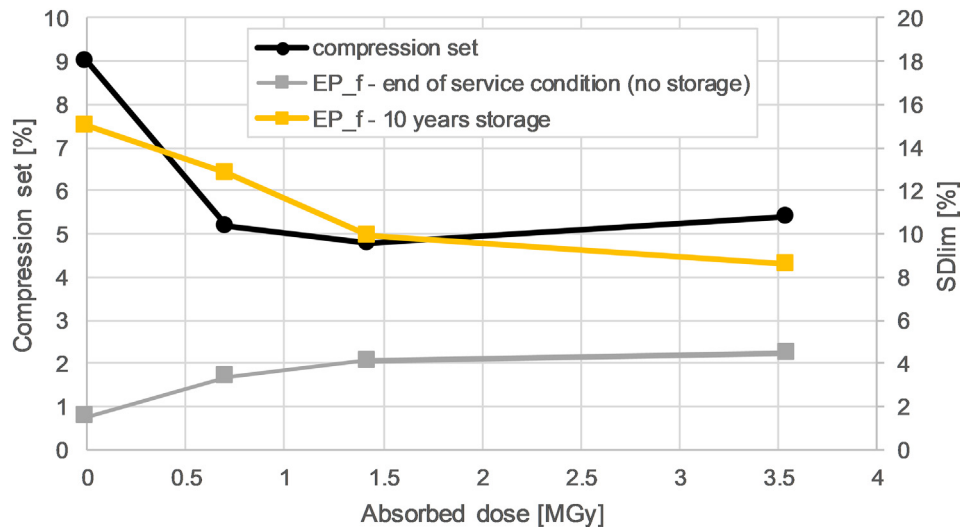
Fig. 16. Compression set and SD$_{lim}$ (squeeze degree value associated with leakage initiation) trends as function of the absorbed dose level.

in the end-of-service (no-storage) condition. Therefore, even though compression set might be a way too simple indicator of sealing performance in general, especially when complex interactions are present, it might still be considered, at least in our case scenario, a qualitative indicator of long-term functional performance.

In addition, functional end-point curves showed an admissible squeeze degree that is almost insensitive to variations of the service time for high values of the service time itself (over 107 days).

Overall, the safe area showed to be very limited for high service times and reasonably extended for lower service times. Specifically, assuming to reach an optimal squeeze degree, the 15 days default service time of SPES showed to be very safe with respect to both the failure conditions. For example, 30, 45 or even 60 days of service time, even though corresponding to two to four times the default service time, seem reasonably safe conditions if the squeeze degree is maintained (approximately) between 24 and 18% respectively.

6. Conclusions

Radioactive environments are a very critical application for sealing components. To the authors' knowledge, there are currently no specific design and maintenance procedures for O-rings applied in nuclear facilities. In addition, the effects of neutron radiation on gasket materials and structural components in general are quite undocumented compared to the effects of γ radiation. In this context, our study proposes a novel approach for O-ring life estimation for this kind of applications. This approach was applied for studying the O-rings of the gate valves of the TIS target chamber of the SPES facility at the Laboratori Nazionali di Legnaro of INFN. Even though the concluding life prediction map is a concise and effective way to present results, many steps had to be carried out to achieve this outcome:

- mechanical characterization at different irradiation levels of the material for the O-ring (EPDM) selected in [2];
- functional characterization of the O-ring at different irradiation levels;
- end-points definition as function of O-ring squeeze degree, service time and storage time;
- gate-valve O-ring life prediction map.

Uniaxial tensile tests data of EPDM at different irradiation levels taken from Zenoni et al. [2], were processed to extract average stress-strain curves and strain at break values. The material showed important stiffening and embrittlement at higher absorbed dose levels and thus

the stress-strain curves and the strain at break values were found to be very dependent on the service time. Furthermore, aging tests, performed at 100 °C environment for 15 days, showed that thermal aging has no significant influence on the stress-strain relationship and on the strain at break values.

Concurrently, as testified by compression set tests, the radiation lead to an enhanced elastic response (i.e. its recovery at unloading after prolonged load) in all the irradiated specimens, and the result is interpreted as a consequence of an increased crosslink density, which leads to an overall stabilization of the material mechanical performances. Considering our case scenario, compression set confirmed being a qualitative indicator of long-term sealing (functional) O-ring performance.

O-rings irradiation campaigns were performed at the TRIGA Mark II reactor of the University of Pavia and the irradiated specimens were then submitted to further experimental testing with dynamic mechanical analyses (DMA) and Vacuum Leak Tests (VLT). Interestingly, DMA tests showed that the slope of the rubbery plateau of the master curves presents a much stronger sensitivity to the absorbed dose level than the glass transition temperature. VLT allowed a limit squeeze degree for leakage initiation to be identified.

VLT were also modelled via finite element method (FEM) to correlate the limit squeeze degree to the contact pressure distributions between O-ring and groove. This approach highlighted that the irradiated O-rings required higher contact pressures in order to prevent leakage than the non-irradiated ones. This is very reasonable since the no-leakage condition is guaranteed when a sealing material fills the cavities and the discontinuities of the groove surface and, in our case scenario, the higher the absorbed dose, the stiffer the O-ring.

The mechanical characterization of the O-ring material led to the definition of a first end-point associated with mechanical failure (breaking condition) and the functional characterization of the O-ring led to the definition of a second end-point associated with functional failure (leakage condition).

Finally, a parametric study by means of FEM simulations was performed on the main O-ring of the most critical sealing component (TIS gate valves) of the SPES system as well. An O-ring life prediction map was constructed by coupling these results with the structural and functional end-points. This map represents an effective tool for design optimization and maintenance scheduling leading to a safer functioning of the whole SPES system. Moreover, considering the huge costs associated with TIS replacement and storage, it is also worth mentioning that extending the TIS service time implies a significant economic

saving. In our case scenario, the life prediction map suggested a possible major enhancement of the TIS service time over the prescribed 15 days.

Acknowledgements

Data availability

The raw data required to reproduce these findings cannot be shared at this time due to technical or time limitations. The processed data required to reproduce these findings cannot be shared at this time due to technical or time limitations.

Authors' contribution

All the authors contributed writing specific parts and overall revisioning of the paper.

Battini D.: corresponding author, wrote the paper, FEM simulations, interpretation of results.

Donzella G.: scientific supervision of the project.

Avanzini A.: FEM simulations.

Zenoni A.: scientific supervision of the project.

Ferrari M.: dosimetry calculations.

Donzella A.: dosimetry calculations.

Pandini S.: experimental testing for material characterization.

Bignotti F.: experimental testing for material characterization.

Andrighetto A.: scientific supervision of the project.

Monetti A.: experimental testing for leakage characterization.

References

[1] G. Prete, A. Andrighetto, M. Manzolaro, S. Corradetti, D. Scarpa, M. Rossignoli, A. Monetti, M. Lollo, The SPES project at the INFN-Laboratori Nazionali di Legnaro, EPJ Web Conf, 2014.

[2] A. Zenoni, F. Bignotti, A. Donzella, G. Donzella, M. Ferrari, S. Pandini, A. Andrighetto, M. Ballan, S. Corradetti, M. Manzolaro, A. Monetti, M. Rossignoli, D. Scarpa, D. Alloni, M. Prata, A. Salvini, F. Zelaschi, Radiation resistance of elastomeric O-rings in mixed neutron and gamma fields: testing methodology and experimental results, Rev. Sci. Instrum. 88 (2017)https://doi.org/10.1063/1.5011035.

[3] R. Flitney, Seals and Sealing Handbook, Elsevier, 2015.

[4] Eriks, Sealing Elements - Technical Handbook O-rings, Eriks, 2013 1–255www.eriks.info.

[5] S.G. Burnay, J.W. Hitchon, Prediction of service lifetimes of elastomeric seals during radiation aging, J. Nucl. Mater. 131 (1985) 197–207.

[6] V. Plaček, T. Kohout, V. Hnát, B. Bartoníček, Assessment of the EPDM seal lifetime in nuclear power plants, Polym. Test. 28 (2009) 209–214, https://doi.org/10.1016/j.polymertesting.2008.12.005.

[7] F. Le Lay, Study on the lifetime of EPDM seals in nuclear-powered vessels, Radiat. Phys. Chem. 84 (2013) 210–217, https://doi.org/10.1016/j.radphyschem.2012.05.008.

[8] C.P. Porter, J.P. Bezzina, F. Clegg, M.D. Ogden, Polymeric seal degradation in nuclear power plants: determination of physical and mechanical properties, J. Appl. Polym. Sci. 135 (2018) 1–9, https://doi.org/10.1002/app.45814.

[9] C.P. Porter, R. Edge, M.D. Ogden, Polymeric seal degradation in nuclear power plants: effect of gamma radiation on sealing properties, J. Appl. Polym. Sci. 134 (2017) 2–9, https://doi.org/10.1002/app.44618.

[10] P. Pourmand, L. Hedenqvist, A.M. Pourrahimi, I. Furó, T. Reitberger, U.W. Gedde, M.S. Hedenqvist, Effect of gamma radiation on carbon-black-filled EPDM seals in water and air, Polym. Degrad. Stab. 146 (2017) 184–191, https://doi.org/10.1016/j.polymdegradstab.2017.10.008.

[11] R.O. Bolt, J.D. Carrol, Radiation Effects on Organic Materials, Acad. Press. Inc., New York, 1963.

[12] A. Rivaton, J. Arnold, Structural modifications of polymers under the impact of fast neutrons, Polym. Degrad. Stab. 93 (2008) 1864–1868, https://doi.org/10.1016/j.polymdegradstab.2008.07.015.

[13] A. Rivaton, L. Lao, J. Arnold, Fast neutron irradiation effects on organic polymers: suitability for dosimetry purposes? Radiat. Phys. Chem. 80 (2011) 89–93, https://doi.org/10.1016/j.radphyschem.2010.08.007.

[14] P. Beynel, P. Maier, H. Schônbacher, For Nuclear Research Compilation of Radiation Damage Test Data Part III: Materials Used Around High-energy Accelerators, Cern - Yellow Rep, 1982.

[15] D.B. Pelowitz, MCNPX User's Manual, Los Alamos National Laboratory, LA-CP-11-00438, 2005.

[16] F.H. Attrix, Introduction to Radiological Physics and Radiation Dosimetry, WILEY-VCH Verlag GmbH & Co., KGaA, 2004https://doi.org/10.1002/9783527617135.

[17] K. Ambrožič, G. Žerovnik, L. Snoj, Computational analysis of the dose rates at JSI TRIGA reactor irradiation facilities, Appl. Radiat. Isot. 130 (2017) 140–152, https://doi.org/10.1016/j.apradiso.2017.09.022.

[18] A. Ferrari, P.R. Sala, A. Fassò, J. Ranft, FLUKA: A Multi-particle Transport Code, 2005.

[19] L. Laboratory, Triga Mark II MCNP Model, Univ. Pavia, Italy, 2015.

[20] A. Andrighetto, S. Corradetti, M. Manzolaro, A. Monetti, D. Scarpa, S. R., F. Bignotti, G. Donzella, M. Ferrari, S. Pandini, A. Zenoni, D. Alloni, M. Prata, A. Salvini, SPES-Note-WPB06 04 0004/RDS-SPES, https://www.lnl.infn.it/~spes_target 2017.

[21] A. International, ASTM D395-14: Standard Test Methods for Rubber Property — Compression Set, ASTM Int., 2003https://doi.org/10.1520/D0395-03R08.2.

[22] A. International, ASTM D1414-94 (03): Standard Test Methods for Rubber O-rings, ASTM Int., 2003https://doi.org/10.1520/D1414-15.2.

[23] B.W.L.M. Sessink, N.F. Verster, Design of elastomer O-ring vacuum seals, Vacuum 23 (1973) 319–325.

[24] R. Yamamoto, K. Watanabe, K. Hanashima, ICONE23-1610 Endurance Test Report of Rubber Sealing Materials for the Containment Vessel, 2015.

[25] R. Yamamoto, K. Ootani, K. Hanashima, The Behavior of a Compression set of Rubber Gaskets for Containment Vessels in the Case of Radiation Timing, 2016 1–5.

[26] N.G. McCrum, C.P. Buckley, C.B. Bucknall, Principles of Polymer Engineering, Oxford University Press, 1998.

[27] R.S. Marlow, A general first invariant hyperelastic constitutive model, in: B. Muhr (Ed.), Const. Model. Rubber III, Swets & Zeitlinger, 2003.

[28] K.T. Gillen, R. Bernstein, M.H. Wilson, Predicting and confirming the lifetime of o-rings, Polym. Degrad. Stab. 87 (2005) 257–270, https://doi.org/10.1016/j.polymdegradstab.2004.07.019.